ASM Sc. J., 12, Special Issue 4, 2019 for ICSE2018, 10-18

# Statistical Analysis of Graphene Layer on Gold-based Surface Plasmon Resonance-Kretschmann Configuration using FDTD and Taguchi Method

Nur Akmar Jamil[1], P. Susthitha Menon[1*], Z.A. Noor Faizah[1] and P.R. Apte[2]

[1]*Institute of Microengineering and Nanoelectronics (IMEN), Universiti Kebangsaan Malaysia (UKM) 43600 Bangi, Selangor, Malaysia*

[2]*Indian Institute of Technology(IIT), Powai, Mumbai, India*

Accurate screening methods have significant implications for kidney health. While the existing methods for identifying specifics samples are often inaccurate and time-consuming, the need for sensitive and precise biosensor is highly demanded. The development of sensors for commonly clinical biomarkers, if properly optimized, can help to address the problem. Here, the optimum design of surface plasmon resonance (SPR) which is recommended by the L9 Taguchi method was reported. In order to achieve the smallest possible full-width-at-half- maximum (FWHM) and the reflectance intensity (Rmin), four input parameters which include the wavelength (λ) and the thickness of three other parameters; Chromium (Cr), Gold (Au) and graphene were varied for the optimization purposes. The SPR biosensor was designed using the Kretschmann configuration through the Lumerical Finite-Difference-Time-Domain (FDTD) simulator. Taguchi method reveals that wavelength parameter holds a significant effect on the device performance. Upon optimization, the FWHM and Rmin show an improvement to the device's sensitivity as much as 5.37% and 38.93% respectively.

**Keywords:** ANOVA, FDTD, Kretschmann Configuration, L9 Taguchi, Surface Plasmon Resonance

## I. INTRODUCTION

Technological advances are growing rapidly but dragging human life towards destruction. Increased youth generation with chronic illness proves that a healthy lifestyle is no longer a priority. Chronic kidney disease (CKD) which is caused by the scarce albumin is one of the major contributors to health problems with global prevalence around 10-26% (Chaudhari, *et al.,* 2017; Menon *et al.,* 2018; Menon *et al.,* 2019a). In 2014, Malaysia has shown a growth rate as much as 56.4% patients that are diagnosed with CKD where the data gathered are within the 10 years of period (Bujang *et al.*, 2017; Rizal *et al.,* 2017). The number of patients with CKD is also forecasted to be increased by twofold in 2040 if it is not properly controlled. This disquieting phenomenon has made Malaysia now as the top seventh country with the highest number of dialysis treatment percentage in the world (Bujang *et al.,* 2017). Numerous approaches were made to effectively evaluate kidney functioning of a person who has potential on suffering the kidney disease beside educating them on a healthy lifestyle. The most common clinical examination is by measuring one's physiological parameters such as creatinine, pH, glucose, and urea in blood or urine using detection method such as amperometry and spectrophotometric (Lee *et al.*, 2000; Soldatkin *et al.,* 2003; Luo & Do, 2004; Kaushik *et al.*, 2009). The advancement method in biosensor such as CO2 gas electrode and gas selective electrodes is also available for urea detection. Although the methods are accurate, the monitors are actually large, complicated and vulnerable to the interference leading to the need of an additional electrode to compensate the electrical interference is

*Corresponding author's e-mail: susi@ukm.edu.my

compulsory and hence spike the total cost of the biosensor (Swati *et al.*, 2010; Chaudhari *et al.*, 2017). For that reason, a precise and cost-effective urea biosensor is very critical to make medical costs affordable to every community.

The surface plasmon resonance (SPR) was introduced and recent studies focus on various types of surface plasmon resonance (SPR) biosensor design for sensing purposes like hazardous gaseous (Prabhash *et al.*, 2017), heavy metal ions (Wu & Lin, 2005), drug molecules (Pernites *et al.*, 2011), and immune-sensing (Ashley *et al.*, 2017). Urea sensing also was extensively explored in various technological topologies using SPR-based sensor (Dindar *et al.*, 2011; Verma & Gupta, 2014). Compared to other methods, the SPR biosensor has exceptional capabilities where it is a fast-optical and label-free detection tool for refractive index deviations at a very close area of a thin metal layer (Nguyen *et al.,* 2015; Gan *et al.*, 2019). Kretschmann configuration has been utilized preeminently in the SPR system, which principally includes an analyte sensing surface, a prism and a glass slide with a thin metal film where the plasmon filed is excited (Jamil *et al.*, 2017a). Technically, when a plane-polarized light beam passes through the prism, total internal reflection (TIR) will occur and an evanescent wave (EW) is formed at a certain critical angle of incident angle (Tarumaraja *et al.*, 2016; Said *et al.*, 2015a). This happens due to the energy from the incident light being transfer onto the surface plasmons (Menon *et al.*, 2019b). A significant decline in the reflectivity and a sharp dip was forms in the SPR response curves demonstrate the minimum reflectivity based on the TIR at the metal-dielectric interface (Said *et al.*, 2016). The existence of the analyte in the sample can be seen through the shifting mode in the incident angle or through the optical wavelength since the SPR are sensitive to the variations of the refractive index on the sensing surface layer (Jamil *et al.*, 2017b). The performance of SPR biosensor is at optimum when it has the highest sensitivity, selectivity and long-term stability of metal and sensing (Jamil *et al.*, 2018a).

These works are the extension studies from our previous work in (Jamil *et al.*, 2018b). Here, we optimize the Kretschmann SPR-based sensor using the L9 orthogonal array (OA) of the Taguchi method (Siew Mei *et al.,* 2018). The numerical simulation was initially designed using the Lumerical finite-domain-time-domain analysis (FDTD)-based simulators (*FDTD Solutions | Lumerical's Nanophotonic FDTD Simulation Software*). Numerous works prove that the optimizations using Taguchi in designing the experiments are cost-effective which agrees with the purpose of these works to find the best recipe of process parameters in achieving the smallest possible full-width-at-half- maximum (FWHM) and reflectance intensity (Rmin) at a lower cost without scarifying the accuracy of the device (A *et al.*, 2016; Mitra *et al.*, 2016). Taguchi effectively concludes the best combination of control factors through the analysis of variance (ANOVA) and Signal-to-Noise ratio (SNR) analysis (Lee, Lin & Yen, 2017; Tarumaraja *et al.*, 2019). In order to attain the smallest possible FWHM and Rmin, Smaller-the-Better (STB) of Taguchi's quality characteristic was utilized so that the sensitivity and accuracy of the device can be increased. In this work, four critical parameters were selected to be varied at three levels. The parameters include the wavelengths (λ), the thickness of chromium ($T_{Cr}$), the thickness of the gold layer ($T_{Au}$), and the thickness of graphene layers ($T_{Graphene}$). The efficacy of the Taguchi method can be seen through the increased percentage of device performance after the optimization process takes place.

## II. MATERIALS AND METHOD

The design and analysis phases of a virtual SPR-based biosensor using the Lumerical's FDTD Solutions software follows as in (Jamil *et al.*, 2018b; Jamil *et al.*, 2018c) except the utilization of different analyte and variations in input parameters for device optimization. Initially, the biosensor is formed in the high optical solver environment for capturing light interaction with the anticipated wavelength scale. Accurate setting and conformal meshing using a mesh override region are essential to simulate the plasmonic structures of metal geometries (Said *et al.*, 2017). Then, the optical parameter is established to design the biosensor. Here, the plane-wave source is set as a Bloch (periodic type) at a desired optical wavelength (Jamil *et al.*, 2018a). In order to find the source angle (θ) which is capable to excite the SPR mode, a parameter is engulfed within 36° to 80° of the incident angle (Said *et al.,* 2015b).

### *A. Numerical Modeling*

Figure 1 illustrated the simulated design of graphene-based SPR biosensor. In this work, Kretschmann prism configuration is used as a platform for SPR sensing where

the development of SPR biosensor includes four main components; BK7 glass, chromium layer (Cr), gold layer (Au) and the graphene layer. Note that, all related values of the refractive index and the extinction coefficient for the glass and chromium layer are obtained from the Bionavis Navi SPR database (Mohamad *et al.*, 2019). The complex refractive index of the gold layer is listed in Table 1. The data are measured at three optical wavelengths that excite the SPR mode; 632.8 nm, 670 nm and 785 nm. The thickness of the graphene in this work is determined by the formula L × 0.34 nm, where L is the number of graphene layers. The complex refractive index of graphene in visible light is given by:

$$n = 3 + i\frac{C}{3} \quad (1)$$

where C is the value of the constant implied by the opacity measurement (C = 5.446 μm-1) and $\lambda$ is the optical wavelength.

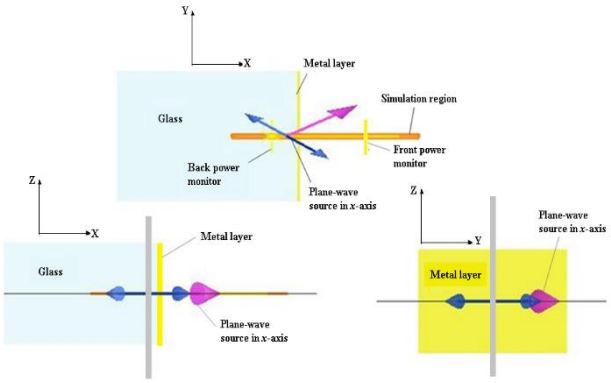


Figure 1. The XY, XZ and YZ view of simulated FDTD diagrams for SPR biosensor-based graphene using Kretschmann (Said *et al.*, 2015c)

Table 1. The complex refractive index of a gold layer

| Metal | Wavelength, $\lambda$ (nm) | Refractive Index, n (RI) | Extinction Coefficient, $k$ |
|---|---|---|---|
| Gold (Au) | 632.8 | 0.1968 | 3.2478 |
| | 670 | 0.1741 | 3.6123 |
| | 785 | 0.1836 | 4.5871 |

### *B. Taguchi Orthogonal L9 Array Method*

In L9 Taguchi method, the variations of process parameters in findings the best combination of factors level are used to achieve the optimal device performance at a smaller number of experiments. A total of nine experiments each for Rmin and FWHM were simulated in this work considering of four process factors known as factor A (wavelength, λ), factor B (chromium thickness, $T_{Cr}$), factor C (gold thickness, $T_{Au}$) and factor D (graphene layer thickness, $T_{Graphene}$). These factors are varied at three levels in order to find the optimum value that can reduce the Rmin and FWHM. The process factors and their respective level values are listed in Table 2.

Table 2. Factors and levels

| Sym. | Factor (nm) | Level 1 | Level 2 | Level 3 |
|---|---|---|---|---|
| A | Wavelength, λ | 663 | 670 | 785 |
| B | Thickness of Chromium, $T_{Cr}$ | 0.5 | 1.5 | 2.0 |
| C | Thickness of Gold, $T_{Au}$ | 40 | 45 | 50 |
| D | Thickness of Graphene, $T_{Graphene}$ | 0.34 | 0.68 | 1.02 |

Since the aim of the experiments is to have the lowest output of Rmin and FWHM, the device is optimized using the Taguchi's Smaller-the-Better (STB) quality characteristics. The layout of the experiment can be seen in previous works (Jamil *et al.*, 2019). The Signal-to-Noise ratio (SNR) of STB characteristic ($\eta$STB) and the analysis of variance (ANOVA) for Rmin and FWHM are calculated once the simulations are completed. The $\eta$STB is defined as in equation (2) where n is the number of experiment and $y_i$ is the simulation result for Rmin and FWHM (Tseng *et al.*, 2013).

$$\eta_{STB} = -10\ \log\left(\frac{1}{n}\sum_{i=1}^{n} {y_i}^2\right) \quad (2)$$

## III. RESULTS AND DISCUSSION

The analysis of the virtual graphene-based SPR using the Lumerical FDTD software was first benchmarked with the experimental result. This is to confirm the efficacy of the virtual device before it is optimized. From the result, the virtual device demonstrates a good agreement with the experimental output data. This can be seen in Figure 2 where a sharp dip of reflection intensity (≈1.0 a.u.) at an

incident angle of ≈45° can be seen at both numerical and experimental reflectance curve in the same simulation environment; 50 nm Au/Graphene on BK7 at 670 nm wavelength in the dielectric medium air. The reflectance intensity difference between the curves was less than 5%. The red colour curve represents the experimental result and the blue curve represent the numerical result.

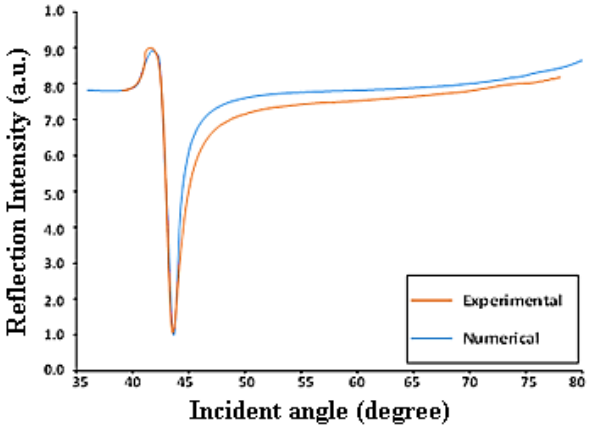


Figure 2. SPR curve of 50nm Au-Graphene based SPR biosensor at wavelength 670 nm

### *A. Analysis of Graphene-based Surface Plasmon Resonance Sensor*

The signal-to-noise ratio (SNR) of smaller-the-better (STB) L9 Taguchi quality characteristic was utilized to improve the sensitivity of the biosensor by reducing the FWHM and Rmin value. Four process factors which include the wavelength (λ), chromium thickness ($T_{Cr}$), gold thickness ($T_{Au}$) and graphene layer thickness ($T_{Graphene}$) were varied at three levels making the total of nine experiments required to find the best combination of process factor's level for optimum device performance. Figure 3 shows the reflectance curves of nine experiments established by L9 Taguchi method while the simulation results of Rmin and FWHM are listed in Table 3. From the figure, it can be seen that the wavelength escalates as the slopes of reflectivity shifted to a lower angle. The narrowest curves happen at experiment number 7, 8 and 9 when the wavelength is set constant at 785 nm. This explains that the results of FWHM were also the lowest at these levels. The result of FHWM at experiment number 7, 8 and 9 is 1.254°, 1.4746°, and 1.4076° respectively. Rmin, on the other hand, has the lowest result at experiment number 1, 2 and 4 with the value of 0.0131, 0.0122 and 0.0047 respectively.

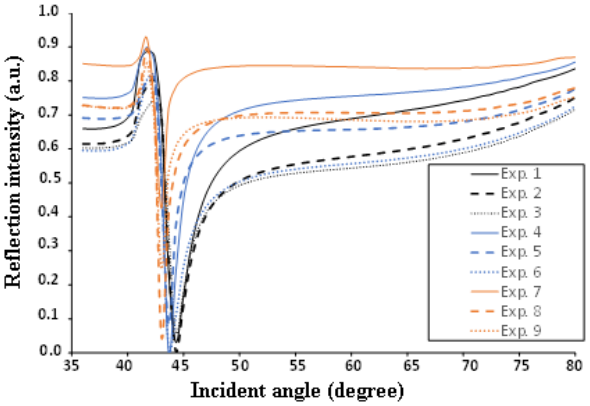


Figure 3. Reflectance curve of SPR biosensor-based graphene for Taguchi analysis

Table 3. FWHM and Rmin results

| Exp. no. | L9 OA Experimental Layout | | | | FWHM | Rmin |
|---|---|---|---|---|---|---|
| | A | B | C | D | | |
| 1 | 1 | 1 | 1 | 1 | 3.6304 | 0.0131 |
| 2 | 1 | 2 | 2 | 2 | 3.5868 | 0.0122 |
| 3 | 1 | 3 | 3 | 3 | 3.2739 | 0.0627 |
| 4 | 2 | 1 | 2 | 3 | 2.1713 | 0.0047 |
| 5 | 2 | 2 | 3 | 1 | 1.823 | 0.0571 |
| 6 | 2 | 3 | 1 | 2 | 3.646 | 0.0318 |
| 7 | 3 | 1 | 3 | 2 | 1.254 | 0.3633 |
| 8 | 3 | 2 | 1 | 3 | 1.4746 | 0.0470 |
| 9 | 3 | 3 | 2 | 1 | 1.4076 | 0.1571 |

### *B. Signal-to-Noise Ratio (SNR) and ANOVA Results*

The SNR was measured right after the simulations of the nine experiments were completed. The SNR is obtained to study the most influence level parameters to the device performance. Hence, the performance characteristics of the graphene-based biosensor are at the optimum level when the SNR value is at the highest level (Afifah Maheran et al. 2014; Yorek et al. 2018). The results of SNR for FWHM and Rmin at each level of the experiment are tabulated in Table 4. From the table, experiment results at set number 4 and 7 give the highest SNR value for Rmin and FWHM analysis correspondingly. Since the Taguchi method is orthogonal, the SNR results of each level can be separated and studied. The SNR contribution at each level of process factor can be seen clearly in Table 5 and plotted as in Figure 4. The SNR analysis for FWHM suggested that the best combination

factors are A at level 3, B at level 2, C at level 3 and D at level 1 while the best combination factors for optimum Rmin are A at level 2, B at level 1, C at level 2 and D at level 3. Note that the selection of levels was based on the highest SNR value. The greater the SNR contribution, the better the quality characteristic of the graphene-based SPR biosensor.

Table 4. SNR analysis for FWHM and Rmin

| Exp. no. | SNR STB, $\eta_{STB}$ (dB) | |
|---|---|---|
| | FWHM | Rmin |
| 1 | -11.20 | 37.69 |
| 2 | -11.09 | 38.30 |
| 3 | -10.30 | 24.07 |
| 4 | -6.73 | 46.60 |
| 5 | -5.22 | 24.89 |
| 6 | -11.24 | 29.99 |
| 7 | -1.97 | 8.84 |
| 8 | -3.37 | 26.60 |
| 9 | -2.97 | 16.12 |

Table 5. SNR analysis for FWHM and Rmin

| Factor | FWHM | | | Rmin | | |
|---|---|---|---|---|---|---|
| | Level 1 | Level 2 | Level 3 | Level 1 | Level 2 | Level 3 |
| A | -10.86 | -7.73 | -2.77 | 33.35 | 33.83 | 17.19 |
| B | -6.63 | -6.56 | -8.17 | 31.04 | 29.93 | 23.39 |
| C | -8.60 | -6.93 | -5.83 | 31.43 | 33.67 | 19.27 |
| D | -6.46 | -8.10 | -6.80 | 26.23 | 25.71 | 32.42 |

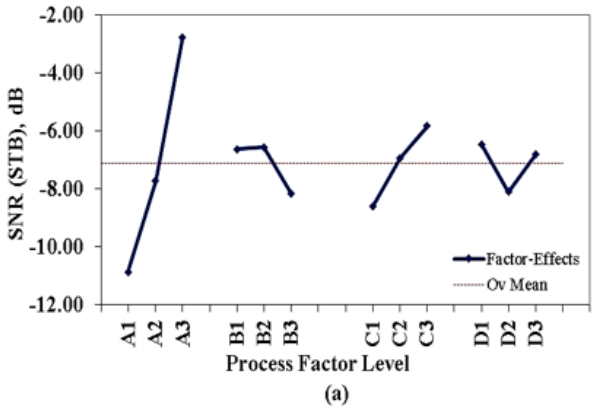


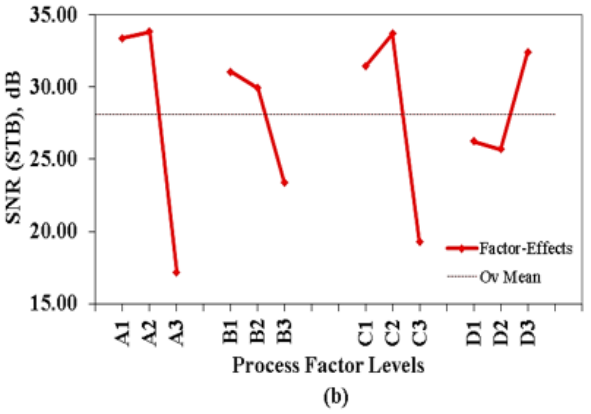


Figure 4. SNR (STB) graph for a) FWHM and b) Rmin

*1. Confirmation Test*

The confirmation tests were done to verify the suggested process factors give better result after the optimization took place. The suggested level of each factor is tabulated in Table 6. The percentage of factor effect shown in Table 6 specified that factor A is the dominant factor for both FWHM and Rmin. This means that any changes made to factor A will affect the device performance significantly. Therefore, selection of a proper optical wavelength to excite the device is vital for designing a sensitive SPR-based biosensor as compared to other process factors. Final results of FWHM and Rmin are shown in Table 7. The FWHM was improved by 5.37% after the optimization while Rmin was improved by almost 40%. However, both output parameters did not share the same combination of the optimum factor's level. This means that the finest combination of factors for the lowest possible FWHM does not signify the lowest Rmin and vice versa. Hence, an additional simulation was done to find the trade-off between the FWHM and Rmin. Both factor effects were then compared and the new level of factors was selected based on the highest percentage of factor effect. Consequently, both performance parameters are reduced and identified using the same optimized process factors. The final results of combined factors (FWHM x Rmin), A3B1C2D3 gives the FWHM value of 0.8602° which is further reduced as compared to the individual optimization. However, the result of the combined factor for Rmin increases but still in the allowable range.

Table 6. Optimum factor combination for FWHM and Rmin

| Factor | FWHM | | Rmin | |
|---|---|---|---|---|
| | Level | % Factor Effect | Level | % Factor Effect |
| A | 3 | 82.54 | 2 | 49.66 |
| B | 2 | 4.09 | 1 | 9.42 |
| C | 3 | 9.67 | 2 | 33.18 |
| D | 1 | 3.70 | 3 | 14.69 |

Table 7. Predicted and confirmation results of FWHM and Rmin

| Performance Parameter | | Best Level | Prediction | Optimized Result | % Improvement |
|---|---|---|---|---|---|
| FWHM | | A3, B2, C3, D1 | 1.19° | 1.1261° | 5.37 |
| Rmin | | A2, B1, C2, D3 | 0.00768 | 0.00469 | 38.93 |
| FWHM x Rmin | FWHM | A3, B1, C2, D3 | | 0.8602° | |
| | Rmin | A3, B1, C2, D3 | | 0.08159 | |

## IV. CONCLUSION

The optimization of process factors for the lowest possible FWHM and Rmin was successfully completed. This work proves that proper selection of the design factors is very crucial in designing the finest SPR biosensor. The lowest possible FWHM and the bigger reflection spectra are desired in the SPR biosensor because a narrower and deeper resonance peak allows detecting the resonance shift effectively. We found that the optical wavelength has the most substantial effect to both FWHM and Rmin which also justify that the prediction made by the Taguchi method is indisputable. The optimization using Taguchi method prior to fabrication delivers a methodology with lessening time and cost besides providing an understanding of the effect of process factors on the device performance.

## V. ACKNOWLEDGMENT

This work was funded by Universiti Kebangsaan Malaysia (UKM) with Grant no. DIP-2016-022 and GUP-2016-062. The use of computational and experimental sources was supported by the Institute of Microengineering and Nanoelectronics (IMEN), UKM, Kulim Hi-Tech Sdn Bhd and Bionavis Ltd.

## VI. REFERENCES

A, NFZ, Ahmad, I, Ker, PJ, Y, SM, R, MF, Mah, SK & Menon, PS 2016, 'Statistical modelling of 14nm N-Types MOSFET', *Journal of Telecommunication, Electronic and Computer Engineering*, vol. 8, no. 4, pp. 91–95.

Ashley, J, Piekarska, M, Segers, C, Trinh, L, Rodgers, T, Willey, R & Tothill, IE 2017, 'An SPR based sensor for allergens detection', *Biosensors and Bioelectronics*, vol. 88, pp. 109–113.

Bujang, MA, Adnan, TH, Hashim, NH, Mohan, K, Liong, AK, Ahmad, G, Leong, GB, Bavanandan, S & Haniff, J 2017, 'Forecasting the incidence and prevalence of patients with end-stage renal disease in malaysia up to the year 2040', *International Journal of Nephrology*, vol. 2017.

Chaudhari, R, Joshi, A & Srivastava, R 2017, 'pH and Urea Estimation in Urine Samples using Single Fluorophore and Ratiometric Fluorescent Biosensors', *Scientific Reports* , pp. 1–9.

Dindar, B, Karaku, E & Abas, F 2011, 'New urea biosensor based on urease enzyme obtained from helycobacter pylori', *Applied Biochemistry and Biotechnology*, vol. 165, no. 5–6, pp. 1308–1321.

'FDTD Solutions | Lumerical's Nanophotonic FDTD Simulation Software', accessed February 26, 2018.

Gan, SM, Menon, PS, Mohamad, NR, Jamil, NA & Majlis, BY 2019, 'FDTD simulation of Kretschmann based Cr-Ag-ITO SPR for refractive index sensor', *Materials Today: Proceedings*, vol. 7, pp. 668–674.

Jamil, NA, Menon, PS, Said, FA, Tarumaraja, KA,

Mei, GS & Majlis, BY 2017a, 'Graphene-based surface plasmon resonance urea biosensor using Kretschmann configuration', in *Proceedings of the 2017 IEEE Regional Symposium on Micro and Nanoelectronics, RSM 2017,* pp. 112-115.

Jamil, NAB, Menon, PS, Mei, GS, Shaari, S & Majlis, BY 2017b, 'Urea biosensor utilizing graphene-MoS2 and Kretschmann-based SPR', in *IEEE Region 10 Annual Proceedings/TENCON*, pp. 1973-1977.

Jamil, NA, Menon, PS, Shaari, S, Mohamed, MA & Majils, BY 2018a, 'Taguchi optimization of surface plasmon resonance-kretschmann biosensor using FDTD', in *IEEE International Conference on Semiconductor Electronics, Proceedings, ICSE*, pp. 65-68

Jamil, NA, Mei, GS, Khairulazdan, NB, Thiagarajah, SP, Hamzah, AA, Majlis, BY & Menon, PS 2018b, 'Detection of Uric Acid Using Kretschmann-based SPR Biosensor with MoS2-Graphene', in *2018 IEEE Student Conference on Research and Development (SCOReD)*, IEEE, pp. 1–4.

Jamil, NA, Susthitha Menon, P, Mei, GS & Majlis, BY 2018c, 'Sensitivity enhancement of urea biosensor based on surface plasmon resonance and kretschmann configuration with graphene-MoS2 hybrid structure', *Sains Malaysiana*, vol. 47, no. 5, pp. 1033–1038

Jamil, NA, Khairulazdan, NB, Menon, PS, Md Zain, AR, Hamzah, AA & Majlis, BY 2019, "Graphene-MoS2 SPR-based biosensor for urea detection," *ISESD 2018 - International Symposium on Electronics and Smart Devices: Smart Devices for Big Data Analytic and Machine Learning*, art. no. 8605491.

Kaushik, A, Solanki, PR, Ansari, AA, Sumana, G, Ahmad, S & Malhotra, BD 2009, 'Iron oxide-chitosan nanobiocomposite for urea sensor', *Sensors and Actuators B: Chemical*, vol. 138, pp. 572–580.

Lee, BS, Lin, DZ & Yen, TJ 2017, 'A low-cost, highly-stable surface enhanced raman scattering substrate by si nanowire arrays decorated with au nanoparticles and Au backplate', *Scientific Reports*, vol. 7, no. 1, pp. 1–7.

Lee, W, Kim, S, Kim, T, Lee, KS, Shin, M & Park, J 2000, 'Sol – gel-derived thick-film conductometric biosensor for urea determination in serum', *Analytica Chimica Acta*, vol. 404, pp. 195–203.

Luo, Y & Do, J 2004, 'Urea biosensor based on PANi ( urease ) -Nafion ® / Au composite electrode', *Biosensors and Bioelectronic*, vol. 20, no. June 2003, pp. 15–23.

Menon, PS, Said, FA, Mei, GS, Berhanuddin, DD, Umar, AA, Shaari, S & Majlis, BY 2018, 'Urea and creatinine detection on nano-laminated gold thin lm using Kretschmann-based surface plasmon resonance biosensor', *PLOS ONE*, pp. 1–9.

Menon, PS, Said, FA, Gan, SM, Mohamed, MA, Zain, ARM, Shaari, S & Majlis, BY 2019a, 'High Sensitivity Urea Biosensor using Urease enzyme and Au-based Kretschmann Surface Plasmon Resonance', *Sains Malaysiana*, vol. 48, no. 6, pp. 1179–1185.

Menon, PS, Mulyanti, B, Jamil, NA, Wulandari, C, Nugruho, HS, Gan, SM, Abidin, NFZ, Hasanah, L, Pawananto, RE & Berhanuddin, DD 2019b, 'Sensitivity enhancement of urea biosensor based on surface plasmon resonance and kretschmann configuration with graphene-MoS2 hybrid structure', *Sains Malaysiana*, vol. 48, no. 6, pp. 1259–1265.

Mitra, AC, Jawarkar, M, Soni, T & Kiranchand, GR 2016, 'Implementation of Taguchi Method for Robust Suspension Design', in *Procedia Engineering*.

Mohamad, NR, Mei, GS, Jamil, NA, Majlis, B & Menon, PS 2019, 'Influence of ultrathin chromium adhesion layer on different metal thicknesses of SPR-based sensor using FDTD', *Materials Today: Proceedings*, vol. 7, pp. 732–737.

Nguyen, HH, Park, J, Kang, S & Kim, M 2015, 'Surface plasmon resonance: A versatile technique for biosensor applications', *Sensors (Switzerland)*, vol. 15, no. 5.

Pernites, R, Ponnapati, R, Felipe, MJ & Advincula, R 2011, 'Biosensors and Bioelectronics Electropolymerization molecularly imprinted polymer ( E-MIP ) SPR sensing of drug molecules : Pre-polymerization complexed terthiophene and

carbazole electroactive monomers', *Biosensors and Bioelectronics*, vol. 26, no. 5, pp. 2766–2771.

Prabhash, PG, Haritha, VS, Nair, SS & Pilankatta, R 2017, 'Sensors and Actuators B : Chemical localized surface plasmon resonance based highly sensitive room temperature pH sensor for detection and quantification of ammonia', *Sensors & Actuators: B. Chemical*, vol. 240, pp. 580–585.

Rizal, M, Manaf, A, Surendra, NK, Halim, A, Gafor, A, Hooi, LS & Bavanandan, S 2017, 'Dialysis provision and implications of health economics on peritoneal dialysis utilization : a review from a Malaysian perspective', *International Journal of Nephrology*, vol. 2017, pp. 1–7.

Said, FA, Menon, PS, Shaari, S & Majlis, BY 2015a, 'FDTD Analysis on Geometrical Parameters of Bimetallic Localized Surface Plasmon Resonance-Based Sensor', in *2015 6th International Conference on Intelligent Systems, Modelling and Simulation (ISMS)*, pp. 242–245.

Said, FA, Menon, PS, Kalaivani, T, Mohamed, MA, Abedini, A, Shaari, S, Majlis, BY & Retnasamy, V 2015b, 'FDTD analysis of structured metallic nanohole films for LSPR-based biosensor', in *2015 IEEE Regional Symposium on Micro and Nanoelectronics (RSM)*, IEEE, pp. 1–4.

Said, FA, Susthitha Menon, P, Shaari, S & Majlis, BY 2015c, 'FDTD analysis on geometrical parameters of bimetallic localized surface plasmon resonance-based sensor and detection of alcohol in water', *International Journal of Simulation: Systems, Science and Technology*, vol. 16, no. 4, p. 6.1-6.5.

Said, FA, Menon, PS, Nawi, MN, Md Zain, AR, Jalar, A & Majlis, BY 2016, 'Copper-graphene SPR-based biosensor for urea detection', in *2016 IEEE International Conference on Semiconductor Electronics (ICSE)*, pp. 264–267

Said, FA, Menon, PS, Rajendran, V, Shaari, S & Majlis, BY 2017, 'Investigation of graphene-on-metal substrates for SPR-based sensor using finite-difference time domain', *IET Nanobiotechnology*, vol. 11, no. 8, pp. 981–986.

Siew Mei, G, Radiah Binti Mohamad, N, Akmar Binti Jamil, N, Yeop Majlis, B & Susthitha Menon, P 2018, 'Pengoptimuman sensor resonans plasmon permukaan berdasarkan Kretschmann dengan kaedah Taguchi (optimization of Kretschmann based on surface plasmon resonance sensor using Taguchi method)', *Sains Malaysiana*, vol. 47, no. 10, pp. 2565–2571.

Soldatkin, AP, Montoriol, J, Sant, W, Martelet, C & Jaffrezic-renault, N 2003, 'A novel urea sensiti v e biosensor with extended dynamic range based on recombinant urease and ISFETs', *Biosensors and Bioelectronic*, vol. 19, no. 2, pp. 131–135.

Swati, M, Hase, NK & Srivastava, R 2010, 'Nanoengineered optical urea biosensor for estimating hemodialysis parameters in spent dialysate', *Analytica Chimica Acta*, vol. 676, no. 1–2, pp. 68–74.

Tarumaraja, KA, Menon, PS, Said, FA, Jamil, NA, Ehsan, AA, Shaari, S, Majlis, BY & Jalar, A 2016, 'FDTD numerical analysis of SPR sensing using graphene-based photonic crystal', *Proceedings of IEEE International Conference on Semiconductor Electronics,* pp. 79–81.

Tarumaraja, KA, Susthitha Menon, P, Majlis, Y & Apte, PR 2019, Robust design of Kretschmann plasmonic PCW-based integrated biosensor circuit, *International Journal of Nanoelectronics and Materials*, vol. 12, no. 2, pp. 165-174

Tseng, K-H, Shiao, Y-F, Chang, R-F & Yeh, Y-T 2013, 'Optimization of microwave-based heating of cellulosic biomass using taguchi method', *Materials*, vol. 6, no. 8, pp. 3404–3419.

Verma, R & Gupta, BD 2014, 'A novel approach for simultaneous sensing of urea and glucose by SPR based optical fiber multianalyte sensor.', *The Analyst*, vol. 139, no. 6, pp. 1449–55.

Wu, C & Lin, L 2005, 'Utilization of albumin-based sensor chips for the detection of metal content and characterization of metal – protein interaction by surface plasmon resonance', *Sensors and Actuators*

*B: Chemical*, vol. 110, no. 2, pp. 231–238.

Yorek, M, Malik, RA, Calcutt, NA & Vinik, A 2018, 'Editorial diabetic neuropathy : new insights to early diagnosis and treatments', *Journal of Diabetes Research*, vol. 2018, pp. 3–6.